Soliton Microcombs Multiplexing Using Intracavity-Stimulated Brillouin Lasers

Hao Zhang,[1] Teng Tan,[1] Hao-Jing Chen,[2,3] Yan Yu,[2,3] Wenting Wang,[4] Bing Chang,[1] Yupei Liang,[1] Yanhong Guo,[1] Heng Zhou,[1] Handing Xia,[5] Qihuang Gong,[2] Chee Wei Wong,[4] Yunjiang Rao,[1,6,*] Yun-Feng Xiao,[2,†] and Baicheng Yao[1,‡]

[1]*Key Laboratory of Optical Fibre Sensing and Communications (Education Ministry of China), University of Electronic Science and Technology of China, Chengdu 611731, China*

[2]*State Key Laboratory for Mesoscopic Physics and Frontiers Science Center for Nano-optoelectronics, School of Physics, Peking University, Beijing 100871, China*

[3]*T. J. Watson Laboratory of Applied Physics, California Institute of Technology, Pasadena, California 91125, USA*

[4]*Fang Lu Mesoscopic Optics and Quantum Electronics Laboratory, University of California, Los Angeles, California 90095, USA*

[5]*Research Center of Laser Fusion, China Academic of Engineering Physics, Mianyang 621900, China*

[6]*Research Centre for Optical Fiber Sensing, Zhejiang Laboratory, Hangzhou 310000, China*

(Received 16 August 2022; accepted 17 March 2023; published 12 April 2023)

Solitons in microresonators have spurred intriguing nonlinear optical physics and photonic applications. Here, by combining Kerr and Brillouin nonlinearities in an over-modal microcavity, we demonstrate spatial multiplexing of soliton microcombs under a single external laser pumping operation. This demonstration offers an ideal scheme to realize highly coherent dual-comb sources in a compact, low-cost and energy-efficient manner, with uniquely low beating noise. Moreover, by selecting the dual-comb modes, the repetition rate difference of a dual-comb pair could be flexibly switched, ranging from 8.5 to 212 MHz. Beyond dual-comb, the high-density mode geometry allows the cascaded Brillouin lasers, driving the co-generation of up to 5 space-multiplexing frequency combs in distinct mode families. This Letter offers a novel physics paradigm for comb interferometry and provides a widely appropriate tool for versatile applications such as comb metrology, spectroscopy, and ranging.

DOI: 10.1103/PhysRevLett.130.153802

Owing to the high quality (Q) factor and small mode volume, light-matter interaction is dramatically enhanced in optical microresonators, which makes them become a captivating platform for nonlinear optical physics and photonic applications [1,2]. In particular, the microcavity-enhanced Kerr effect has led to the realization of frequency combs in a miniature platform [3–5]. In recent years, the blooming of soliton microcomb technology [6–10] has enabled versatile out-of-lab advances in applications ranging from optical communications [11–13], optical atomic clock [14,15], optical sensing [16], to dual-comb spectroscopy [17,18]. Especially, microcomb multiplexing methods are particularly appealing for applications such as dual-microcomb spectroscopy and LiDAR [19–22]. However, commonly these methods require either an additional external laser [23] or a fast electro-optic modulator [24] to obtain a second pump light for dual-soliton microcomb generation. The complexity and cost associated with the operation of multiple narrow-linewidth laser or high-bandwidth modulator devices limit the simplicity of the system and the mutual coherence between the comb outputs.

Stimulated Brillouin scattering (SBS), a process that arises from the coherent coupling between optical fields and phonons, is another intriguing nonlinear effect in microcavities [25]. Resulting from its highly effective gain and narrow band features, the SBS process in microresonators has been used to generate intracavity ultranarrow linewidth laser and further led to versatile applications in low-noise microwave signal generation [26], Brillouin gyroscope [27], and soliton generation [28].

Here, we demonstrate the spatial multiplexing of Kerr soliton microcombs in a single over-modal microresonator using intracavity Brillouin excitations. The intracavity Brillouin lasing not only provides pumping for an additional set of microcomb with naturally narrow linewidths and fixed phase relations to the primary pump light, which enables remarkably high coherence of the dual-comb source; but also eliminates the requirement for additional lasers or modulators, which can significantly simplify the dual-comb system. In such a high-Q silica microcavity supporting rich mode families, besides its own Kerr soliton formation, the pump laser can excite backwardly circulating cascaded Brillouin lasers (BLs) [29–31], when the Brillouin gain regions overlap varied resonances. By carefully controlling the pump laser detuning, these BLs can further work as "new pumps" for generating more soliton microcombs in diverse mode families. This scheme raises a new physical paradigm for soliton multiplexing, and offers

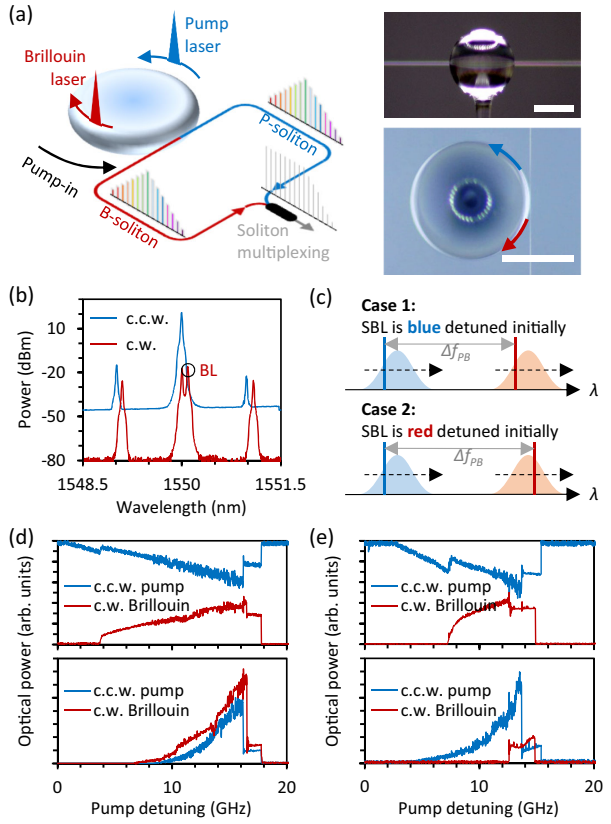

FIG. 1. Conceptual design of the counterpropagating dual soliton. (a) Schematic and micrograph of the microresonator and dual-comb generation. Scale bar: 300 μm. (b) Zoom-in spectrum of the CCW (blue) and CW (red) comb outputs. (c) Two cases of dual-comb generation. (d) and (e) The evolution of the two cases. The top panels show laser power traces while the bottom panels show comb power traces. Blue: CCW, red: CW.

a convenient way to realize dual-comb tools. Moreover, since both the Brillouin lasing [26,28] and the soliton formation are coherently realized in one single cavity, common mode noises are efficiently suppressed [32]. Furthermore, by selecting the excitation mode families of the dual comb, we demonstrate that the repetition rate difference of the generated dual comb could be flexibly switched, ranging from 8.5 to 212 MHz. Finally, owing to the over-modal cavity nature, the BL generation could be cascaded. Therefore, cogeneration of up to 5 spatial-multiplexing soliton frequency combs in distinct mode families is realized.

We utilize the over-modal nature with strong Brillouin scattering of a silica whispering-gallery-mode (WGM) cavity, as Fig. 1(a) shows. The microsphere is fabricated from a commercial optical fiber section using the discharge-sintering technique (Supplemental Material [33], Sec. I) with a diameter of ~600 μm and a Q factor of 1.2×10^8. A tunable external laser (pump laser, PL) is coupled into the cavity via a tapered fiber, circulating in the counterclockwise (CCW) direction. By properly tuning the PL frequency into a cavity resonance, stimulated BL could be generated in the clockwise (CW) direction. Since the free spectral range (FSR) of our cavity is ~110 GHz while the Brillouin shift frequency is of the order of 10 GHz, the PL and the BL are usually located in two distinct mode families. In order to generate Brillouin-Kerr dual-comb, both mode families should exhibit anomalous group velocity dispersion (GVD). When further tuning the PL frequency from blue to red, we achieve single Kerr soliton state in both directions. The coexistence of such Brillouin-Kerr dual soliton is also demonstrated in numerical simulations (see Supplemental Material [33] Sec. III). The PL- and BL-based soliton have different repetition rates, and are easily combined via a fiber coupler to form dual-comb outputs.

The comb signals are collected in both CW and CCW directions, the enlarged spectra around the pump wavelength are shown in Fig. 1(b). The PL and the BL have a wavelength difference of 0.084 nm, which corresponds to the Brillouin shift frequency in silica and suggests the PL and BL belong to different spatial modes. Besides, the first pair of comb lines in the CCW and CW directions also have different wavelengths, verifying that the counterpropagating combs are generated by the PL and the BL, respectively. The process of dual-soliton co-generation is also investigated, and there are two different cases when scanning the PL across different modes [Fig. 1(c)]. The reason is that the initial "Brillouin gain–resonance" overlapping could be varied, while the frequency difference between the PL and the BL (Δf_{PB}) is typically fixed, determined by the material and the cavity geometry. In case 1, the BL is initially generated at the blue-detuned side of the BL mode, and the comb in both directions evolves regularly (i.e., from primary, chaotic, to soliton state in sequence), as shown in Fig. 1(d). While in case 2, the BL is initially generated at the red-detuned (or slightly blue-detuned) region. With the pump laser scanning, the power of the BL gradually increases. Once reaching the Kerr parametric oscillation threshold, soliton burst is triggered [39], as shown in Fig. 1(e). In this measurement, the PL scanning speed is 50 GHz/s and the PL power is fixed at 120 mW. Thanks to the high-Q factor of the cavity and the self-stabilization of the BL [40], the experimentally obtained soliton step existence range reaches 2 GHz. It is noted that the phenomenon of "pump + Brillouin" dual-soliton co-generation is not certain for every mode pair, as the Brillouin gain band may not cover a high-Q resonance with anomalous dispersion.

The co-generated PL-based CCW soliton and the BL-based CW soliton are characterized after generation. The optical spectra are shown in Fig. 2(a). In these two spectra, power of the PL is lower than the BL due to the pump filtering operation. For the steady state shown here, $\Delta f_{\mathrm{PB}} \approx 10.48$ GHz. The soliton spectra are broad, with 3 dB bandwidths of 1.47 and 0.95 THz. Spectrum of the BL-based soliton slightly deviates from the sech^2 shape, which may result from higher order dispersion in the BL

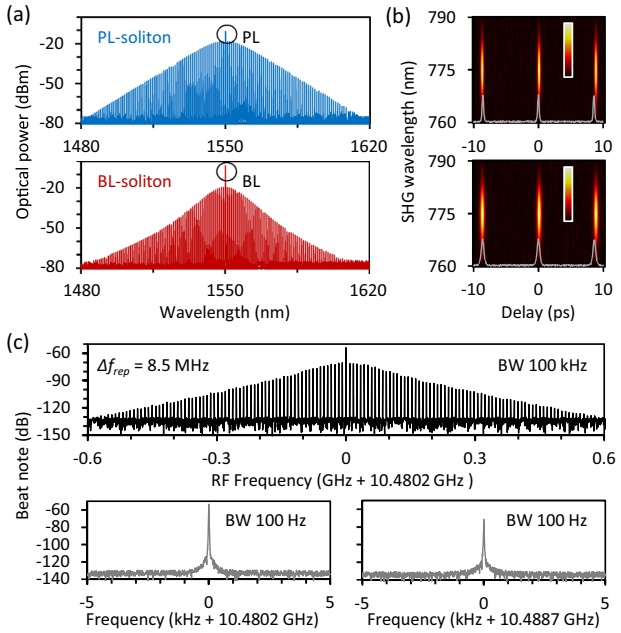

FIG. 2. The co-generated dual soliton. (a) Optical spectra, top and bottom panels: PL- and BL-generated single soliton. (b) FROG maps corresponding to (a). Grey curves show the autocorrelation traces of the two pulse trains. Color bar: normalized pulse intensity. (c) Top panel: Dual-soliton beat note in the rf domain. Central frequency of the electrical comb is 10.4802 GHz, determined by Δf_{PB}. The electrical comb line spacing equals to $\Delta f_{\mathrm{rep}} = 8.5$ MHz. Bottom panels show the enlarged spectra of the pump-Brillouin laser beat note (at 10.4802 GHz) and the first-order comb line pair beat note (at 10.4887 GHz).

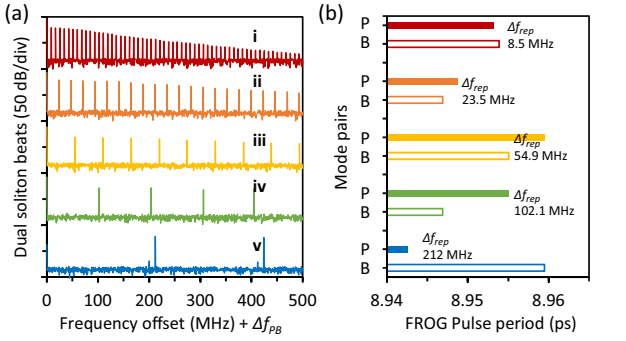

FIG. 3. Switchable dual-soliton beating. (a) Distinct dual-soliton beats when the PL and the BL locate in different modes. Here we only show the single sideband for better clarity. From top to bottom, Δf_{rep} increases from 8.5 to 212 MHz. (b) Measured pulse periods of the dual-soliton pairs. Here the solid and the hollow columns show the pulse periods of the PL-based soliton (P) and the BL-based (B), for case ***i*** to ***v***.

mode family [41]. Using the second harmonic generation (SHG)-based autocorrelation technique, we also measured frequency-resolved-optical-gating (FROG) maps of the two soliton combs [Fig. 2(b)]. The retrieved pulse duration of the CCW and the CW soliton is 215 and 332 fs, respectively, matching their optical spectra well. Three soliton pulses are shown in a single FROG frame, with a temporal window of 20 ps. For the CCW soliton, the repetition period is 8.9532 ps, while for the CW soliton, the repetition period is 8.9539 ps, verifying the repetition frequency difference between the two combs.

After combining two solitons together, we measure the dual-comb beat notes in Fig. 2(c). Mixing of the two solitons forms an electrical comb in the radio frequency (rf) domain. The strongest central beat note locates at 10.4802 GHz (Δf_{PB}). This is the beat between the PL and the BL at mode number $\mu = 0$. On both sides of this beating line, other comb lines demonstrate the one-to-one beat notes between the two frequency combs. The spacing of the electrical comb is equal to the repetition frequency difference ($\Delta f_{\mathrm{rep}} = 8.5$ MHz) between the two soliton combs. Since $\Delta f_{\mathrm{PB}} \gg \Delta f_{\mathrm{rep}}$, there is no spectral aliasing. By zooming the rf spectrum in, we characterize the two beat notes, at 10.4802 GHz ($\mu = 0$, Δf_{PB}) and 10.4887 GHz ($\mu = 1$, $\Delta f_{\mathrm{PB}} + \Delta f_{\mathrm{rep}}$). Signal to noise ratio (SNR) of the pump-Brillouin beat is higher than 60 dB; meanwhile, SNR of the beat note between the first order comb line pairs is approaching 50 dB. Noise analyses are shown in the Supplemental Material [33], Sec. IV.

Since the over-modal microresonator has many co-existing mode families, such dual-comb multiplexing could appear in varied mode pairs. The group index of these mode families is different, offering chances to obtain distinct Δf_{rep} in dual-comb interference. This unique property enables varied dual-comb beat notes in a single microresonator. Experimentally, different mode pairs could be selected by carefully tuning the PL wavelength into a specific mode and exciting the BL in another specific mode. Figure 3(a) shows 5 distinct beat notes in the rf domain by exciting dual-soliton in varied mode pairs. From top to bottom, the PL wavelength is located at 1550.024, 1550.013, 1550.816, 1551.21, and 1550.72 nm. Δf_{rep} of the five cases are 8.5, 23.5, 54.9, 102.1, and 212 MHz, correspondingly. We also note that Δf_{rep} could be even higher, up to several GHz, but once Δf_{rep} is higher than 300 MHz, the limited Δf_{PB} may cause beat aliasing in the rf domain. Since the repetition rates and pulse periods are related to the group refractive index of the PL and BL mode, the specific PL-BL mode pair for the above 5 cases are varied. Δf_{rep} of the five cases are confirmed by the pulse periods obtained from the FROG measurements, as Fig. 3(b) shows. The pulse periods of the PL solitons are 8.9532, 8.9491, 8.9588, 8.9549, and 8.9423 ps; meanwhile the pulse periods of the BL solitons are 8.9539, 8.9473, 8.9549, 8.9468, and 8.9591 ps. We note that in our microsphere geometry supporting more than 100 transverse mode families, to accurately identify the specific mode-to-mode pairs is difficult, but high-density mode distribution

still offers a unique chance to find diverse dual-soliton combinations, which enables the Δf_{rep} of a dual-comb tool to be switchable.

This over-modal nature not only supports switchable dual-soliton beat notes, but also provides a possibility of cascaded BL generation if there are 3 or more resonances with a uniform spacing of ≈10.48 GHz and sufficiently high Q factors. Once all modes exhibit anomalous dispersion, > 2 soliton multiplexing can be realized in the single microresonator, by carefully selecting the pumping mode and combining the comb outputs from both the CW and the CCW directions. Such an operation further enriches the diversity of the microcomb device.

In the experiments, the multiplexed microcombs are collected from both the CW and CCW directions through a fiber coupler. The spectra around the pump laser wavelength are shown in Fig. 4(a). From top to bottom, we excite 1, 2, 3, and 4 BLs by carefully tuning the wavelength of a single PL. Each Brillouin excitation is driven by the optical signal ∼10.48 GHz above it and belongs to a distinct mode family. These lasers travel in opposite directions one by one, for example, the PL propagates in the CCW direction, while the 1st, 2nd, 3rd, and 4th order BL go in CW, CCW, CW, and CCW directions, respectively. All the Brillouin lasers are capable of generating Kerr combs in principle. Figure 4(b) demonstrates the optical spectra of 2, 3, 4, and 5 Kerr comb multiplexing, from top to bottom. The rf spectrum of the comb states in the 0–400 MHz band is shown in Fig. 4(c). Among the four comb states, state ***i***, ***ii***, and ***iv*** feature low noise. Nevertheless, we do not claim that every comb here is in the single soliton state, because the mixed measurement of interferogram for 5 comb multiplexing needs > 40 GHz bandwidth in heterodyne characterization, and the mixed temporal trace of them is too complex to be well distinguished. For case ***iii***, the rf noise is high, meaning there is at least one chaotic comb inside.

Taking advantage of the propagating direction difference of the intracavity frequency combs, we can easily measure the two-comb interferograms, by further down mixing the beat notes electrically using a 10 GHz sinusoidal signal. From top to bottom, Fig. 4(d) plots the temporal traces of several dual-comb pairs. Here the colored arrows present the comb circulating directions, corresponding to Fig. 4(a). For instance, in case *i*, both the CCW comb (driven by the PL) and the CW comb (driven by the first order BL) are in a single soliton state, temporal delay per round-trip of them is 117.65 ns ($\Delta f_{\mathrm{rep}} = 8.5$ MHz, see Fig. 2), as the blue curve plots. In case ***ii***, the CCW circulating comb driven by the PL is a single soliton, but there are four solitons in the CCW circulating comb driven by the second order BL, we see thus each cluster has 4 pulses in the down-mixed signal. In case ***iii***, we know the CCW circulating comb driven by the PL is a single soliton (it appears first), and the copropagating dual-comb interference delivers equidistant pulse train

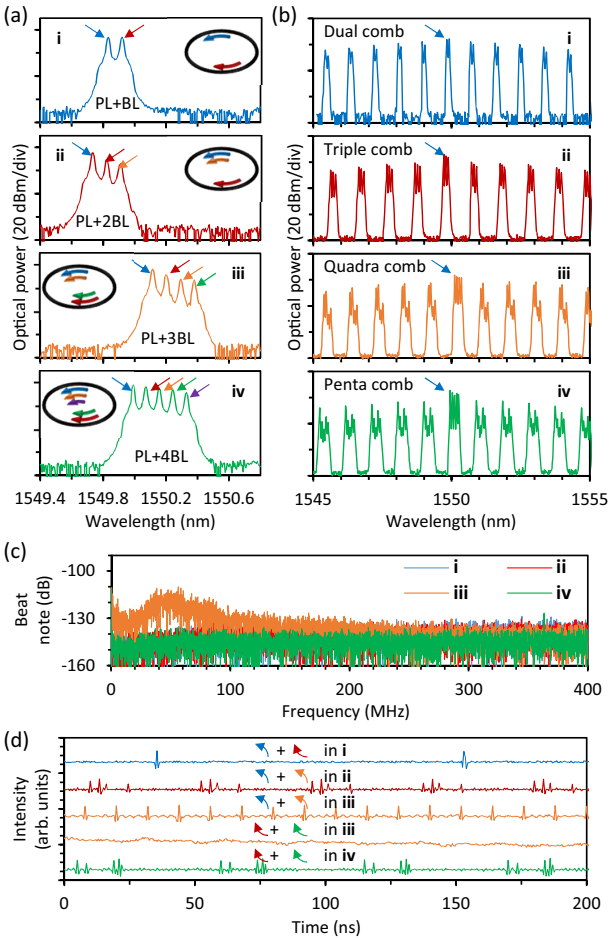

FIG. 4. Microcombs multiplexing using cascaded Brillouin lasers. (a) Single PL generates cascaded BLs in distinct mode families, from ***i*** to ***iv***, up to 4 BLs are generated. Colored arrows: PL and cascaded BLs. (b) Co-excitation of multicomb in a single microresonator. From ***i*** to ***iv***, in every bunch one can see 2–5 comb lines. The equally distributed line-to-line spacing is determined by the Δf_{PB}. (c) Measured rf spectrum (0–400 MHz) of case ***i*** to ***iv***. (d) Dual-comb interferograms in case ***i*** to ***iv***. In the dual-soliton heterodyne, stable pulse clusters demonstrate a stable Δf_{rep}.

(period 12 ns, $\Delta f_{\mathrm{rep}} = 83.3$ MHz). We speculate that the comb generated by the 2nd BL is also a single soliton. On the other hand, the interferogram in the CW direction demonstrates chaotic features, suggesting that there is at least a noisy comb in the CW direction. Finally, in case ***iv***, we observe 5 pulses in each cluster. The versatile dual-comb signal collected from either the "CW" or the "CCW" direction of such a multiplexed comb system offers a flexible tool for advanced applications such as optical frequency domain reflectometers [42,43] and vernier spectrometers [44,45].

In summary, by using a single PL and its stimulated BL excitations, *in situ* generation and spatial multiplexing of soliton microcombs in a single over-modal microresonator are demonstrated. Via tuning the PL frequency, both forwardly and backwardly circulating Kerr solitons could

be simultaneously excited. These two solitons have excellent mutual coherence, with an optical frequency offset of ~10.48 GHz, offering a scheme to realize dual comb interferometry conveniently. Careful mode selection enables the repetition rate difference of a dual-comb pair to be flexibly switchable, in a range of 8.5 to 212 MHz, experimentally. Moreover, we demonstrate that the BL generation could be cascaded, suggesting a way to co-generate up to 5 space-multiplexing frequency combs in varied mode families. This practically flexible and easily scalable method helps to improve our understanding about Brillouin-Kerr nonlinear interactions in microcavities, and inspires the simplification and integration of microcomb systems. It may show unique potential to extend the capabilities of microcomb interferometry based platforms in wide applications such as metrology, spectroscopy, and LiDAR.

We thank technical supports from Professor Qi-Fan Yang and Dr. Qi-Tao Cao at Peking University. We acknowledge financial support from the National Key Research and Development Program of China (2021YFB2800602), the National Natural Science Foundation of China (61975025, U2130106, 11825402, 11904339, and 12293051), the State Key laboratory (2022GZKF002), and the National Postdoctoral Innovation Talent Support Program of China (BX20220056).

H. Z., T. T., H.-J. C., Y. Y., and W. W. contributed equally to this work. B. Y. and Y.-F. X. led this study. H. Z., T. T., and W. W. contributed the experimental investigations, Y. Y. and H.-J. C. contributed the theoretical analysis. B. C., Y. L., Y. G., and H. X. built the experimental setup and fabricated the devices. All authors processed and analyzed the results. B. Y., Y. R., Y.-F. X., H.-J. C., and C. W. prepared the manuscript.

*Corresponding author.
yaobaicheng@uestc.edu.cn
†Corresponding author.
yjrao@uestc.edu.cn
‡Corresponding author.
yfxiao@pku.edu.cn

[1] D. Armani, T. Kippenberg, S. Spillane, and K. Vahala, Nature (London) **421**, 925 (2003).
[2] J. Liu, F. Bo, L. Chang, C.-H. Dong, X. Ou, B. Regan, X. Shen, Q. Song, B. Yao, W. Zhang *et al.*, Sci. China Phys. Mech. Astron. **65**, 1 (2022).
[3] P. Del'Haye, A. Schliesser, O. Arcizet, T. Wilken, R. Holzwarth, and T. J. Kippenberg, Nature (London) **450**, 1214 (2007).
[4] T. J. Kippenberg, R. Holzwarth, and S. A. Diddams, Science **332**, 555 (2011).
[5] H.-J. Chen, Q.-X. Ji, H. Wang, Q.-F. Yang, Q.-T. Cao, Q. Gong, X. Yi, and Y.-F. Xiao, Nat. Commun. **11**, 2336 (2020).
[6] T. Fortier and E. Baumann, Commun. Phys. **2**, 153 (2019).
[7] B. Shen, L. Chang, J. Liu, H. Wang, Q.-F. Yang, C. Xiang, R. N. Wang, J. He, T. Liu, W. Xie *et al.*, Nature (London) **582**, 365 (2020).
[8] C. Xiang, J. Liu, J. Guo, L. Chang, R. N. Wang, W. Weng, J. Peters, W. Xie, Z. Zhang, J. Riemensberger *et al.*, Science **373**, 99 (2021).
[9] Z. Lu, H.-J. Chen, W. Wang, L. Yao, Y. Wang, Y. Yu, B. Little, S. Chu, Q. Gong, W. Zhao *et al.*, Nat. Commun. **12**, 3179 (2021).
[10] L. Chang, S. Liu, and J. E. Bowers, Nat. Photonics **16**, 95 (2022).
[11] P. Marin-Palomo, J. N. Kemal, M. Karpov, A. Kordts, J. Pfeifle, M. H. Pfeiffer, P. Trocha, S. Wolf, V. Brasch, M. H. Anderson *et al.*, Nature (London) **546**, 274 (2017).
[12] B. Corcoran, M. Tan, X. Xu, A. Boes, J. Wu, T. G. Nguyen, S. T. Chu, B. E. Little, R. Morandotti, A. Mitchell *et al.*, Nat. Commun. **11**, 2568 (2020).
[13] Y. Geng, H. Zhou, X. Han, W. Cui, Q. Zhang, B. Liu, G. Deng, Q. Zhou, and K. Qiu, Nat. Commun. **13**, 1070 (2022).
[14] S. B. Papp, K. Beha, P. Del'Haye, F. Quinlan, H. Lee, K. J. Vahala, and S. A. Diddams, Optica **1**, 10 (2014).
[15] Z. L. Newman, V. Maurice, T. Drake, J. R. Stone, T. C. Briles, D. T. Spencer, C. Fredrick, Q. Li, D. Westly, B. R. Ilic *et al.*, Optica **6**, 680 (2019).
[16] T. Tan, Z. Yuan, H. Zhang, G. Yan, S. Zhou, N. An, B. Peng, G. Soavi, Y. Rao, and B. Yao, Nat. Commun. **12**, 6716 (2021).
[17] I. Coddington, N. Newbury, and W. Swann, Optica **3**, 414 (2016).
[18] N. Picqué and T. W. Hänsch, Nat. Photonics **13**, 146 (2019).
[19] A. Dutt, C. Joshi, X. Ji, J. Cardenas, Y. Okawachi, K. Luke, A. L. Gaeta, and M. Lipson, Sci. Adv. **4**, e1701858 (2018).
[20] M. Yu, Y. Okawachi, A. G. Griffith, N. Picqué, M. Lipson, and A. L. Gaeta, Nat. Commun. **9**, 1869 (2018).
[21] P. Trocha, M. Karpov, D. Ganin, M. H. Pfeiffer, A. Kordts, S. Wolf, J. Krockenberger, P. Marin-Palomo, C. Weimann, S. Randel *et al.*, Science **359**, 887 (2018).
[22] M.-G. Suh and K. J. Vahala, Science **359**, 884 (2018).
[23] M.-G. Suh, Q.-F. Yang, K. Y. Yang, X. Yi, and K. J. Vahala, Science **354**, 600 (2016).
[24] E. Lucas, G. Lihachev, R. Bouchand, N. G. Pavlov, A. S. Raja, M. Karpov, M. L. Gorodetsky, and T. J. Kippenberg, Nat. Photonics **12**, 699 (2018).
[25] W. Loh, A. A. Green, F. N. Baynes, D. C. Cole, F. J. Quinlan, H. Lee, K. J. Vahala, S. B. Papp, and S. A. Diddams, Optica **2**, 225 (2015).
[26] J. Li, H. Lee, and K. J. Vahala, Nat. Commun. **4**, 2097 (2013).
[27] J. Li, M.-G. Suh, and K. Vahala, Optica **4**, 346 (2017).
[28] Y. Bai, M. Zhang, Q. Shi, S. Ding, Y. Qin, Z. Xie, X. Jiang, and M. Xiao, Phys. Rev. Lett. **126**, 063901 (2021).
[29] D. Braje, L. Hollberg, and S. Diddams, Phys. Rev. Lett. **102**, 193902 (2009).
[30] K. Jia, X. Wang, D. Kwon, J. Wang, E. Tsao, H. Liu, X. Ni, J. Guo, M. Yang, X. Jiang *et al.*, Phys. Rev. Lett. **125**, 143902 (2020).
[31] C. Qin, J. Du, T. Tan, B. Chang, K. Jia, Y. Liang, W. Wang, Y. Guo, H. Xia, S. Zhu *et al.*, Laser Photonics Rev. 2200662 (2023).
[32] Q.-F. Yang, X. Yi, K. Y. Yang, and K. Vahala, Nat. Photonics **11**, 560 (2017).

[33] See Supplemental Material at http://link.aps.org/supplemental/10.1103/PhysRevLett.130.153802 for details of the fabrication process, theoretical models, numerical simulations, and experimental methods, which includes Refs. [34–38].
[34] R. Y. Chiao, E. Garmire, and C. H. Townes, Phys. Rev. Lett. **13**, 479 (1964).
[35] D. Korobko, I. Zolotovskii, V. Svetukhin, A. Zhukov, A. Fomin, C. Borisova, and A. Fotiadi, Opt. Express **28**, 4962 (2020).
[36] E. Obrzud, S. Lecomte, and T. Herr, Nat. Photonics **11**, 600 (2017).
[37] X. Yi, Q.-F. Yang, X. Zhang, K. Y. Yang, X. Li, and K. Vahala, Nat. Commun. **8**, 14869 (2017).
[38] C. Deakin, Z. Zhou, and Z. Liu, Opt. Lett. **46**, 1345 (2021).
[39] H. Zhou, Y. Geng, W. Cui, S.-W. Huang, Q. Zhou, K. Qiu, and C. Wei Wong, Light **8**, 50 (2019).
[40] W. Loh, S. B. Papp, and S. A. Diddams, Phys. Rev. A **91**, 053843 (2015).
[41] M. H. Pfeiffer, C. Herkommer, J. Liu, H. Guo, M. Karpov, E. Lucas, M. Zervas, and T. J. Kippenberg, Optica **4**, 684 (2017).
[42] J. Riemensberger, A. Lukashchuk, M. Karpov, W. Weng, E. Lucas, J. Liu, and T. J. Kippenberg, Nature (London) **581**, 164 (2020).
[43] M. Soriano-Amat, H. F. Martins, V. Durán, L. Costa, S. Martin-Lopez, M. Gonzalez-Herraez, and M. R. Fernández-Ruiz, Light **10**, 51 (2021).
[44] Q.-F. Yang, B. Shen, H. Wang, M. Tran, Z. Zhang, K. Y. Yang, L. Wu, C. Bao, J. Bowers, A. Yariv *et al.*, Science **363**, 965 (2019).
[45] B. Wang, Z. Yang, X. Zhang, and X. Yi, Nat. Commun. **11**, 3975 (2020).